Radar database collected over artificial debonding pavement structures during APT at the IFSTTAR's fatigue carrousel

Xavier Dérobert, Vincent Baltazart, Jean-Michel Simonin, C. Norgeot, S. Doué, Olivier Durand, Shreedhar Savant Todkar

Radar database collected over artificial debonding pavement structures during APT at the IFSTTAR's fatigue carrousel

X. Dérobert*, V. Baltazart*, J.-M. Simonin*, C. Norgeot, S. Doué**, Durand O.*, S.S. Todkar***

* university Gustave Eiffel, IFSTTAR, Allée des Ponts et Chaussées, 44344, Bouguenais, France
email: xavier.derobert@ifsttar.fr
** MDS, 29 av. Puvis de Chavannes, 92400 Courbevoie, France
email: christophe@mds-paris.com

Abstract Data interpretation over disbonded pavement structures still remains an open problem for the scientific community. In this paper, the details of a ground-penetrating radar (GPR) database, collected over artificial disbonded areas during an accelerated pavement testing at IFSTTAR's carrousel, are presented. The database will be made available to the scientific communities. It may serve as a reference benchmark for both developing and testing the performance of various processing techniques for either interface detection and characterization, or monitoring purposes. In practice, GPR data have been collected over three artificial defects (tack-free, geotextile and sand-based), which were embedded between the top and the base layers. The data collection was organized in a two-stage experiments and covers the full life-cycle of the pavement structure. During the first stage that took place in 2012-13, data were collected at each of 10k, 50k, 100k, 200k, 250k and 300k loading cycles. The second measurement campaign was performed in 2019 and lasted up to 720k loading cycles. The database merges two types of existing radar technologies and configurations. Two stepped-frequency radar with 1.5 and 4.5 GHz as center frequency and two impulse radar systems, working at 2.6 and 1.5 GHz, were tested during this experiment.

Keywords Ground penetrating Radar, Stepped-frequency Radar, Non-destructive Testing, Database

1 Introduction

Monitoring structural conditions of road is an important issue in many industrial countries (Wright et al. 2014). In order to plan effective road maintenance, the objective is to detect structural distresses, like debonding and reflective cracking, at an early stage and to afford a better sustainability of the pavement structure.

In that frame, the ground-penetrating radar (GPR) is one major non-destructive testing (NDT) technique, widely used for geometrical information (layer thicknesses), as well as for acceptance of works on new roads as for maintenance on existing roads (Al-Qadi et al., 2002 ; Saarenketo, 2009 ; Plati et al., 2012, Lai et al. 2017). Defects in bituminous pavement have been widely studied within their various form by GPR. Indeed, damages, such as moisture barrier, stripping, segregation or cracking have been analyzed in the last decades (Benedetto and Pensa, 2007 ; Krysinski and Sudyka, 2013 ; Maser, 2013 ; Plati and Loizos, 2013).

Nevertheless, limitation of debonding and crack detection can occur while radar wavelengths remain much larger than the thin layer of degradation at the interface of two bituminous layers. As these damages are due to traffic, the herein study has focused on the detectability of different kind of artificial disbonded areas, in a pavement structure test site under a one-scale controlled traffic simulator, by few GPR techniques. The interest of such study is to create a large GPR database while monitoring the evolution of the test structure, available for developing and testing various GPR processing techniques in term of damage level and lateral extension, of the defects at different loading cycles.

The ongoing experiment has prompted since 6 years a lot of related studies, including PhD topics, internal and international collaborative research projects (Simonin et al., 2014 ; Simonin et al., 2016 ; Todkar et al., 2019). Recently, a final series of loading has come to complete this experiment allowing to reach an advanced level of degradation from the point of view of the engineers managing road networks.

The article is organized as follow: after a presentation of the test facility, a pavement fatigue carrousel carrying moving loads, the several GPR techniques tested during the experiment are presented. Then, some raw data (Bscans) are presented as well as some examples of classical processing; At last, the GPR database is presented.

2 The fatigue carrousel

The IFSTTAR's pavement fatigue carrousel is a road traffic simulator unique in Europe by its size (Fig. 1a). It is composed of a carrousel and a test track. The carousel includes 4 arms carrying the moving heavy loads (45 kN on single wheel, 65 kN on twin wheel, tandem or tridem axles) at different speeds (maximum 100 km/h) and at different radius (15.5 to 19.5 m). The pavement test track is a 6 meter width ring with a radius going from 14.5 m to 20.5 m. Usually, it is divided into different test sections, which are simultaneously loaded. Each test section can be the subject of a specific study or represent an alternative pavement design for a comparative study.

a) b)

Fig. 1 Fatigue carrousel at Iffsttar in Nantes: (a) overview, (b) 25 m long section with embedded artificial defects made of A-a) sandy interface, B-b) geotextile and C-c) interface free of tack coat. GPR data collection was focused on the largest defects, i.e., [A,B,C] patches,

A quarter of the test track, namely 25 m, has been dedicated to study detection and monitoring of interface defect by non destructive testing (NDT) methods. The pavement structure consists of two bituminous layers (8 cm thick base layer, and 6 cm thick wearing course), over a granular sub-base. Rectangular patches of materials were incorporated at the interface between the two asphalt layers to create embedded debonding areas. Patches differ by size, location, and materials, namely, sand, textile, tack-coat free interface (Fig. 1b). They were centered on the radius 16 m which corresponds to the load wheel-path of the experiment.

Table 1 summarizes their type and size. Simonin et al. (2012) give an exhaustive description of the test site including the mechanical behavior of bituminous material (Fig. 2).

The rectangular patches marked [A , a] for sand based defects, [B , b] geotextile based defects and [C , c] tack-coat free interfaces, shown in Fig. 1b, represent the defective regions over which the radar data were collected at the different loading stages in the first 2012 series, studied and presented by Simonin et al.

(2014), Simonin et al. (2016) and Todkar et al. (2019). Defects A and a (B and b, C and c respectifely) only differ in size (Tab. 1).

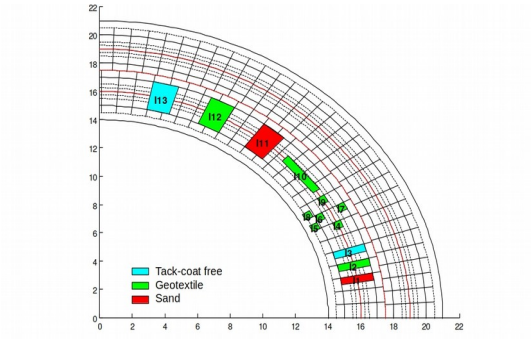

Fig. 2 Location of defect zones (Simonin et al., 2012)

The Geotextile based defects are supposed to represent somehow an ideal case study with the strongest radar signatures. By contrast, the Tack-free defects closely resemble a realistic defective pavement structure for which the two successive layers are not consolidated with some coating.

Table 1 Characteristic of the debonded zones along the test site; in bold, the largest artificial embedded defects on which GPR data were systematically collected.

Name (notation 2012)	Type	Length (m)	Width (m)
I-1 (a)	Sand	0.5	2
I-2 (b)	Geotextile	0.5	2
I-3 (c)	Tack-coat free	0.5	2
I-4 – I-9	Geotextile	0.5	0.5
I-10	Geotextile	3	0.5
I-11 (A)	**Sand**	**1.5**	**2**
I-12 (B)	**Geotextile**	**1.5**	**2**
I-13 (C)	**Tack-coat free**	**1.5**	**2**

One of the major objective of the experiment was to compare the ability of the different GPR techniques to detect artificial defects, to determine their spatial extension, and to follow the evolution of the defects during loading. The experiment started in the spring 2012. Loads of 65 kN were applied on the disbonded area. The fatigue machine was regularly stopped to test the pavement with the different

GPR systems. Thus 300 000 loads were globally applied to the road before the end of July.

Survey of the disbonded zone was possible at different loading times:

– After the construction and before loading (initial state),
– At 8 000 loads, corresponding to the consolidation of the structure,
– at around 50 000, 100 000, 200 00, 250 000 and 300 000 loads.

As the global loading did not reveal clear evolution, either for GPR and complementary NDT techniques, and for road specialists, a second series was programmed. The fatigue carrousel planning, combined to external financing requirements, led to a second series of 400 000 loads in 2019. Survey of the disbonded zone were performed at the following loading times:

– At 310 000 loads, corresponding to a new consolidation of the structure,
– At 396 000, 420 000, 500 000, 550 000, 600 000 and 720 000 loads.

3 GPR techniques

This section presents the GPR systems used during this global campaign. They split into two groups. Ground-coupled impulse radar are described first. As commercial common systems, they correspond to standards for major classical applications. In the second group, stepped-frequency systems are used. The first one is an experimental radar developed at IFSTTAR. The second one is commercial array system which enables to acquire numerous GPR profiles in one pass.

3.1 Ground-coupled impulse radar

Three ground-coupled impulse radar were operated during this global experiment, using GSSI systems; a SIR3000 device associated to a 2.6 GHz antenna during the first series in 2012, and for the 2019 series, a SIR4000 device associated to a 1.5 GHz antenna and a 2.6 GHz StructureScan (Fig. 3).

Such radar systems collect time signals while moving along a defined profile, each time signal (named A-scans) being the results of impulse echoes reflected from every interface towards the receiver antenna. The acquisition of successive A-scans forms a 2D B-scan image of the sub-surface, as illustrated further. For the data collection, raw B-scans were taken at each loading stage, in two major direc-

tions: transverse and longitudinal at the center of the defects. Setup parameters are listed for each B-scan and each loading stage in Section 4.

a) 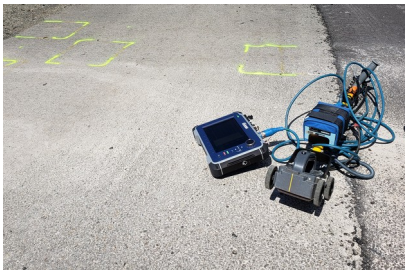 b) 

Fig. 3 Impulse radar: a) SIR4000 model with a 1.5 GHz antenna, b) 2.6 GHz StructureScan

3.2 Bistatic air-coupled stepped-frequency radar

The IFSTTAR's Stepped-Frequency Radar (SFR) used for the experiment over the fatigue carrousel is an experimental Ultra Wide-Band (UWB) radar. Data were collected in the frequency domain within the bandwidth 0.8 GHz–10.8 GHz using a Vector Network Analyzer (VNA) (Dérobert et al., 2001). Inverse Fourier Transform is conventionally used to provide radar data (B-scans) in time domain.

a)  b) 

Fig. 4 a) IFSTTAR's robotic antenna-holder system associated to SFR with UWB antennas (surrounding blue cones are EM absorbing foams). b) 3D-radar system during acquisition

The transmitter and receiver are air-coupled exponentially tapered slot antennas (ETSA) (Diakité et al., 2015) positioned in bi-static configuration with an offset = 20 cm , and at a height $h_{antenna}$ = 40 cm above the pavement surface (Todkar et al., 2019). The useful length of acquisition is about 1.5-1.6 m. Figure 4a shows the robotic antenna-holder system and the RSF during acquisition.

3.3 Stepped-frequency ground-coupled antenna array system

The array system, from 3D-radar manufacturer, is based on a stepped-frequency radar, composed of 21 ground-coupled antennas, arranged to acquire 20 B-scans, spaced by 7.5 cm. The frequency band is ranging from 40 to 3 000 MHz, working with the highest range of frequency, leading after an inverse Fourier transform, to radar data comparable to a 1.5 GHz impulse radar. The array system is dragged behind a vehicle and localized by a RTK centimetric global positioning system (Fig. 4b). Data collection is done with a sampling of 2.5 cm and the width monitoring of each swath is about 1.40 m, inducing three passages.

4 Database format and parameters

Data were collected transversely and longitudinally through the center of defects, For each Bscan, file nomenclature has been defined as:

Freq_Emission_Defect_Orientation_Loading,

where: Freq corresponds to the nominal central frequency (in GHz), Radar type to impulse or stepped-frequency type (Imp or SF), to the name of the defect, to the orientation, specifying if transversal or longitudinal B-scan (T or L) and the loading stage (in kloading) at which the GPR data were collected.

This paper focuses on the major defects (I11, I12 and I13), as most monitored by all the GPR techniques. Setting parameters and B-scans are resumed in Table 2, gathering about 90 B-scans, specifying the radar configuration (ground- or air-coupled), the spatial and sampling frequency and the time range.

Figure 5 presents some examples of GPR profiles done at 600 000 loads on the defect I11 by the 1.5 GHz impulse system and 5.5 GHz stepped-frequency one.

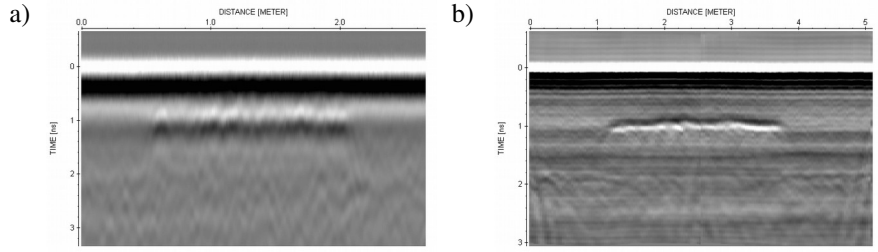

Fig. 5 GPR profiles performed at 600 000 loads done on the defect I11 by a) the 1.5 GHz impulse system (zoom), b) the 5.5 GHz stepped-frequency system (left and right part of the defect)

Table 2 Information about data collected on the fatigue carrousel defects I11, I12 and I13.

GPR system	Central Freq (GHz)	Type impulse	Orientation	File Name	Scan/m	Sampl.	Range (ns)	LP/HP (MHz)	Loading (k)	Nb Files
SIR4000	1.5	Imp	L(T)	1.5_Imp_I11_L_kload	100	1024	7	3000/250	310 / 396 / 420 / 500 / 600 / 720	3*12
3D-radar	1.5	SF	L	1.5_SF_I11_L_kload	67	512	7	3000/40	396 / 500 / 600 / 720	3*4
SIR3000	2.6	Imp	L	2.6_Imp_I11_L_kload	100	1024	8	5000/500	0 / 10 / 50 / 100 / 200 / 250 / 300	3*7
StructureSc.	2.6	Imp	L(T)	2.6_Imp_I11_L_kload	800	256	6	5000/500	310 / 396 / 420 / 500 / 600 / 720	3*12
SFR	5.5	SF	L(T)	5.5_SF_I11_L_kload	50/100	1001	4.9	10800/800	0 / 10 / 50 / 100 / 200 / 250 / 300 310 / 396 / 420 / 500 / 600 / 720	3*19

5 Conclusion

This paper has presented an experiment devoted to the non-destructive testing of artificial debonding areas within pavement structure during an accelerated pavement study on a fatigue carrousel. This experiment enabled to perform some monitoring using several GPR techniques, in order to estimate their ability to detect some embedded artificial defects, to determine their spatial extension, and to follow their evolution during loading.

Then, a total of about 160 B-scans were collected and gathered to constitute a database over the largest defects. The data base is available to the GPR community at https://doi.org/10.25578/N0RXSQ. It may serve as a reference benchmark for both developing and testing the performance of various processing techniques for either interface detection, characterization, or monitoring purposes.

Acknowledgments

The authors would like to thank the technical staff of IFSTTAR Carrousel (S. Trichet, T. Gouy, G. Coirier, Y. Baudry, M. L. Nguyen et J. Blanc).

The first part of the data collection in 2012, has been a contribution of the RILEM technical committee TC241-MCD ("Mechanisms of cracking and debonding in asphalt and composite pavements", www.rilem.org) and the COST action TU1208 ("Civil engineering applications of ground-penetrating radar").

The second part has been supported by the French Research Agency (ANR), the FEREC foundation, and the Ministry of Ecological and Solidarity Transition (MTES) . The authors also thank H.Y. Hui and P.H.G. Ching for experimental help in the frame of a collaboration with Polytechnic university of Hong Kong.

References

Al-Qadi IL, Lahouar S, Loulizi A (2002) Ground penetrating radar evaluation for flexible pavement thickness estimation. Paper presented at the Pavement Evaluation Conference, Roanoke, Virginia, USA

Benedetto A, Pensa S (2007) Indirect diagnosis of pavement structural damages using surface GPR reflection techniques. Journ Appl Geophys, 62:107–123. doi:10.1016/j.jappgeo.2006.09.001

Benedetto A, Tosti F, Ciampoli LB, D'Amico F (2017) An overview of ground-penetrating radar signal processing techniques for road inspections. Sign Proc 132:201–9. doi:10.1016/j.sigpro.2016.05.016.

Buttlar W.G., Chabot A., Dave, E.V., Petit, C., Tebaldi, G. (2018) Mechanisms of cracking and debonding in asphalt and composite pavements State-of-the art, RILEM TC 241-MCD. doi/10.1007/978-3-319-76849-6_5

Dérobert X, Fauchard C, Côte Ph, Le Brusq E, Guillanton E, Dauvignac JY, Pichot Ch (2001) Step frequency radar applied on thin road layers, Journ Appl Geophys 47:317-325. doi:10.1016/S0926-9851(01)00075-1

Diakité C, Fortino N, Dauvignac J-Y (2015) Antenne ETSA "Exponential Tapered Slot Antenna" miniature pour radar à pénétration de surface. Paper presented at journées nationales microondes (JNM 2015), Bordeaux, France. 3-5 June 2015

Krysinski, L, Sudyka, J (2012) Typology of reflections in the assessment of the interlayer bonding condition of the bituminous pavement by the use of an impulse high-frequency ground-penetrating radar. Nondestr Test & Eval 27:219-227. doi:10.1080/10589759.2012.674525

Lai WW, Dérobert X, Annan P (2017) A review of ground penetrating radar application in civil engineering: a 30-year journey from locating and testing to imaging and diagnosis NDT&E Int 96:58-78. doi:10.1016/j.ndteint.2017.04.002.

Maser K (2013) Chapter 2: Laboratory and field evaluations of ground-penetrating radar, in book: Nondestructive Testing to identify Delaminations between HMA layers – Vol. 3. SHRP2 Report S2-R06D-RW-3, 13–19.

Plati C, Georgouli, K, Loizos A (2012) A Review of NDT assessment of road pavements using GPR. RILEM Bookseries, 6:855-860.

Plati C, Loizos A (2013) Estimation of in-situ density and moisture content in HMA pavements based on GPR trace reflection amplitude using different frequencies. Journ Appl Geophys 97:3–10. doi.org/10.1016/j.jappgeo.2013.04.007

Saarenketo, T. (2009). NDT Transportation. Chapter 13 in text book: Ground Penetrating Radar: Theory and Application. Ed- Harry M. Jol. Publisher, Elsevier.

Simonin JM, Baltazart V, Hornych P, KerzréhoJP, Dérobert X, Trichet T, Durand O, Alexandre J, Joubert A (2012) Detection of debonding and vertical cracks with ND techniques during accelerated tests. Paper presented at the 4th International conference on Accelerated Pavement Testing (APT), Davis, California, USA, 19-21 Sept 2012

Simonin JM, Hornych P, Baltazart V, Dérobert X, Thibaut E, Sala J, Utsi V (2014) Case study of detection of artificial defects in an experimental pavement structure using 3D GPR. Paper presented at the 13th GPR'2014 Cong. Proc., Brussels (BE), 30 June-4 July.

Simonin JM, Baltazart V, Le Bastard C, Dérobert X (2016) Progress in monitoring the debonding within pavement structures during accelerated pavement testing on the Ifsttar's fatigue carousel. Paper in the 8th International RILEM Conference, Nantes (FR), 7-9 June.

Todkar S, Le Bastard C, Baltazart V, Ihamouten A, Dérobert X (2019) Performance assessment of SVM-based classification techniques for the detection of artificial debondings within pavement structures from step-frequency A-scan radar data. NDT&E Int 107(102128). doi:10.1016/j.ndteint.2019.102128

Wright D, Baltazart V, Elsworth N, Hamrouche R, Karup J, Lurdes Antunes M, McRobbie S, Merecos V, and Saarenketo T (2014) TRIMM D4.3 Monitoring structural and surface conditions. European Commission DG Research, Tech. Rep. FP7-285119.